

COMPUTING INTERSECTIONS OF IMPLICITLY SPECIFIED PLANE CURVES

SCOTT B. LINDSTROM, BRAILEY SIMS, AND MATTHEW P. SKERRITT

Dedicated to Tomás Domínguez Benavides on the occasion of his 65th birthday

ABSTRACT. We investigate the application of projection algorithms, more specifically the Douglas-Rachford algorithm, to finding points of intersection of two plane curves. We contrast the employment of typical Euclidean reflection with that of Schwarzian reflection. Local convergence near an isolated intersection point is established and the efficacy of the approaches relative to one another and to more classical methods is explored. The extension to curves in higher dimensional space is noted.

1. INTRODUCTION

One of the most significant applications of metric fixed point theory, and the theory of nonexpansive mappings in particular, has been establishing convergence of various projection algorithms for solving the convex feasibility problem:

Find a point satisfying two (or more) convex constraints; that is, in the intersection of two (or more) closed convex subsets of a Hilbert space.

Of special interest to us is the algorithm first proposed in 1956 by Douglas and Rachford [8], for which convergence in the convex case was investigated by Lions and Mercier in 1979 [10] and established in general in [2]. It has long been observed (and exploited) that, despite a lack of theoretical underpinning, the algorithm continues to work well in many situations where at least one of the sets is no longer convex, see for example [1]. We consider one problem which falls into this class.

We investigate the problem of computing a point in the intersection of two analytic plane curves specified implicitly by $f((x, y)) = 0$ and $g((x, y)) = 0$ for $(x, y) \in \mathbb{R}^2$ which we often identify with the complex plane \mathbb{C} . We will also identify the curves themselves with their respective graphs $\mathcal{G}_f := \{(x, y) \in \mathbb{R}^2 : f((x, y)) = 0\}$ and $\mathcal{G}_g := \{(x, y) \in \mathbb{R}^2 : g((x, y)) = 0\}$. Regarding the graphs as constraint sets our problem becomes the non convex feasibility problem of finding a point (x, y) in $\mathcal{G}_f \cap \mathcal{G}_g$. To avoid degeneracies we assume that (x, y) is an isolated point of $\mathcal{G}_f \cap \mathcal{G}_g$ at which the curves have contact of order zero (that is: $\nabla f((x, y))$ and $\nabla g((x, y))$ are both non-zero and not parallel).

In order to better exploit the analytic nature of the curves, we propose to solve the feasibility problem using an adaptation of the Douglas-Rachford algorithm (also

2010 *Mathematics Subject Classification.* 47J25, 47N40.

Key words and phrases. analytic curve, intersection of two curves, Douglas-Rachford algorithm, Schwarzian reflection.

known as *reflect-reflect-average*) [8] in which Euclidean reflections are replaced by Schwarzian reflections.

The Schwarzian reflection of a point $z \in \mathbb{C}$ in an analytic curve K [[11] pages 254 to 257] is $\mathcal{R}_K = \overline{S_K(z)}$, where S_K is the *Schwarz function* for K ; an analytic function such that $S_K(z) = \bar{z}$ for all $z \in K$.

The Schwarz function for $K : k(x, y) = 0$ can often be found by substituting $\frac{z+\bar{z}}{2}$ for x and $\frac{z-\bar{z}}{2i}$ for y in the specification of K and solving for \bar{z} .

Example 1.1. The Schwarz function for the ellipse $E : x^2 + \left(\frac{y}{b}\right)^2 = 1$ can be found by solving

$$\left(\frac{z + \bar{z}}{2}\right)^2 + \left(\frac{z - \bar{z}}{2ib}\right)^2 = 1$$

for \bar{z} , yielding

$$S_E(z) = \frac{1}{1-b^2} \left[(1+b^2)z - 2b\sqrt{z^2 - 1 + b^2} \right].$$

So, the Schwarzian reflection in E is given by

$$\mathcal{R}_E(z) = \overline{S_E(z)} = \frac{1}{1-b^2} \left[(1+b^2)\bar{z} - 2b\sqrt{\bar{z}^2 - 1 + b^2} \right].$$

Similarly, it is readily verified that the Schwarzian reflection in the unit circle $|z| = 1$ is the same as the inversion $z \rightarrow z/|z|^2$. A comparison of Euclidean and Schwarzian reflection in the case of the circle can be seen in figure 1. For the line $\mathbb{L} : \alpha x + \beta y = 0$ Schwarzian reflection coincides with Euclidean reflection in \mathbb{L} ; that is the linear transformation with matrix

$$(1.1) \quad [\mathcal{R}_{\mathbb{L}}] = \frac{1}{\alpha^2 + \beta^2} \begin{pmatrix} \beta^2 - \alpha^2 & -2\alpha\beta \\ -2\alpha\beta & \alpha^2 - \beta^2 \end{pmatrix}.$$

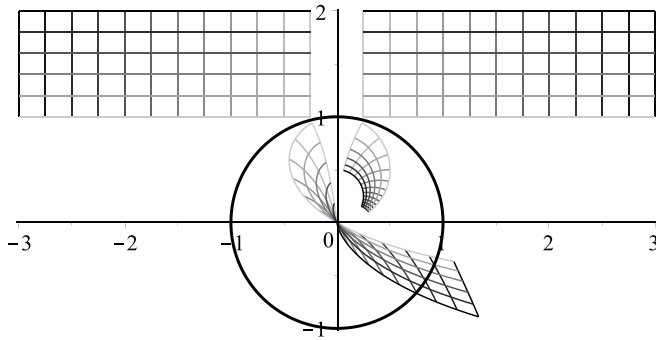


FIGURE 1. Euclidean (left) and Schwarzian (right) reflection.

For more details on Schwarz functions the interested reader is referred to Davis [6].

The Douglas-Rachford algorithm using Schwarzian reflections for finding a point in $\mathcal{G}_f \cap \mathcal{G}_g$ from a given initial point x_0 is the iterative scheme

$$(1.2) \quad x_{n+1} = T(x_n),$$

where $T = T_{\mathcal{G}_f \mathcal{G}_g}$ is the Douglas-Rachford operator

$$(1.3) \quad T_{\mathcal{G}_f \mathcal{G}_g} = \frac{1}{2} (I + \mathcal{R}_{\mathcal{G}_g} \mathcal{R}_{\mathcal{G}_f}).$$

2. LOCAL CONVERGENCE OF THE MODIFIED DOUGLAS-RACHFORD ALGORITHM

For starting points x_0 sufficiently near to $p \in \mathcal{G}_f \cap \mathcal{G}_g$ we apply the theorem of Perron (see, [4] theorem 6.1 or [9] Corollary 4.7.2) to the system of difference equations in (1.2) to show the sequence of Douglas-Rachford iterates converges at a linear rate to p (that is, the iteration scheme (1.2) is exponentially asymptotically stable at p).

To ensure the conditions of Perron's theorem are satisfied we need to show:

- (i) the Douglas-Rachford operator (1.3) is almost linear about p . That is, for x near p

$$(2.1) \quad T_{\mathcal{G}_f \mathcal{G}_g}(x) = p + L_{\mathcal{G}_f \mathcal{G}_g}(x - p) + \Delta,$$

where $L_{\mathcal{G}_f \mathcal{G}_g} : \mathbb{R}^2 \rightarrow \mathbb{R}^2$ is a linear operator and $\|\Delta\| = o(\|x - p\|)$.

and

- (ii) both eigenvalues of $L_{\mathcal{G}_f \mathcal{G}_g}$ have modulus less than 1.

Proof of (i)

To prove (i) it suffices to show for an analytic curve K that near a point p in \mathbb{K} the Schwarz function

$$(2.2) \quad S_K(x) = S_{H_K(p)}(x) + \Delta,$$

where $H_K(p)$ is the tangent (supporting hyperplane) to K at p and $\Delta = \Delta(K, p, x)$ has $\|\Delta\| = o(\|x - p\|)$. As then, for x in a neighbourhood of p we have

$$\begin{aligned} T_{\mathcal{G}_f \mathcal{G}_g}(x) &= \frac{1}{2} [x + R_{\mathcal{G}_g}(R_{\mathcal{G}_f}(x))] \\ &= \frac{1}{2} [x + R_{\mathcal{G}_g}(R_{H_{\mathcal{G}_f}(p)}(x) + \overline{\Delta'})] \\ &= \frac{1}{2} [x + R_{H_{\mathcal{G}_g}(p)}(R_{H_{\mathcal{G}_f}(p)}(x) + \overline{\Delta'}) + \overline{\Delta''}] \\ &= \frac{1}{2} [x + p + R_{H_{\mathcal{G}_g}(p)-p}((p + R_{H_{\mathcal{G}_f}(p)-p}(x - p) + \overline{\Delta'}) - p) + \overline{\Delta''}] \\ &= \frac{1}{2} [x + p + R_{H_{\mathcal{G}_g}(p)-p}(R_{H_{\mathcal{G}_f}(p)-p}(x - p)) + R_{H_{\mathcal{G}_g}(p)-p}(\overline{\Delta'}) + \overline{\Delta''}], \\ &\quad \text{since } R_{H_{\mathcal{G}_g}(p)-p} \text{ is linear} \\ &= \frac{1}{2} [x + p + R_{H_{\mathcal{G}_g}(p)-p}(R_{H_{\mathcal{G}_f}(p)-p}(x - p))] + \frac{1}{2} (R_{H_{\mathcal{G}_g}(p)-p}(\overline{\Delta'}) + \overline{\Delta''}) \end{aligned}$$

So, as required

$$T_{\mathcal{G}_f \mathcal{G}_g}(p) = p + L_{\mathcal{G}_f \mathcal{G}_g}(x - p) + \Delta^*$$

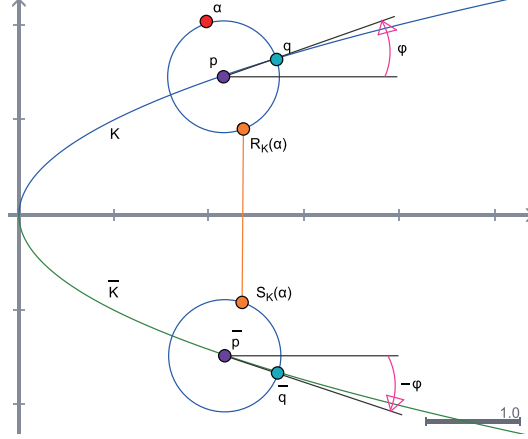


FIGURE 2. Construction of a Schwarz function and Schwarzian reflection

where $L_{\mathcal{G}_f \mathcal{G}_g} := T_{(H_{\mathcal{G}_g}(p)-p)(H_{\mathcal{G}_f}(p)-p)}$ and, since $R_{H_{\mathcal{G}_g}(p)-p}$ is a bounded linear operator, $\Delta^* = \frac{1}{2} \left(R_{H_{\mathcal{G}_g}(p)-p}(\overline{\Delta'}) + \overline{\Delta''} \right)$ has $\|\Delta^*\| = o(\|x - p\|)$.

To establish (2.2) we argue as follows.

Since $S_K(z)$ is analytic it may be expressed as a Taylor series about $p \in K$, so

$$S_K(z) = S_K(p) + S'_K(p)(z - p) + \Delta = \bar{p} + e^{-2\phi i}(z - p) + \Delta,$$

where $|\Delta| = O(|z - p|^2)$ and ϕ is the angle between $H_K(p)$, the tangent to K at p , and the real axis. To see this, refer to figure 2, from which we infer $|S'_K(p)| = 1$ and $\arg(S'_K(p)) = -2\phi$, also see [11], page 255.

Thus

$$\mathcal{R}_K(z) = p + e^{2\phi i} \overline{(z - p)} + \overline{\Delta} = \overline{(z - p)e^{-\phi i} e^{\phi i}} + p + \overline{\Delta}$$

which we recognise as

$$\mathcal{R}_K(z) = R_{H_K(p)}(z) + \overline{\Delta} \quad (\text{see [11], exercise 30(i), page 265}).$$

We now turn to the *proof of (ii)*; $L_{\mathcal{G}_f \mathcal{G}_g}$ is the Douglas-Rachford operator for two non parallel lines; the translated tangents $H_{\mathcal{G}_f}(p) - p$ and $H_{\mathcal{G}_g}(p) - p$, meeting at the origin. We will take these to be $\mathbf{L}_1 : \alpha x + \beta y = 0$ and $\mathbf{L}_2 : Ax + By = 0$ so by (1.3)

$$T_{\mathbf{L}_1 \mathbf{L}_2} = \frac{1}{2} \left(I + \mathcal{R}_{\mathbf{L}_2} \mathcal{R}_{\mathbf{L}_1} \right)$$

which, via (1.1), has matrix

$$[T_{\mathbf{L}_1 \mathbf{L}_2}] = \frac{\psi}{\Delta} \begin{pmatrix} \psi & \omega \\ -\omega & \psi \end{pmatrix},$$

where $\psi = \alpha A + \beta B$, $\omega = \alpha B - \beta A$ and $\Delta = (\alpha^2 + \beta^2)(A^2 + B^2)$. The eigenvalues of $[T_{\mathbf{L}_1\mathbf{L}_2}]$ are $\frac{\psi}{\Delta}(\psi \pm i\omega)$ both of which have modulus squared equal to

$$\begin{aligned} \frac{\psi^2}{\Delta^2}(\psi^2 + \omega^2) &= \frac{(\alpha A + \beta B)^2 ((\alpha A + \beta B)^2 + (\alpha B - \beta A)^2)}{(\alpha^2 + \beta^2)^2 (A^2 + B^2)^2} \\ &= \frac{(\alpha A + \beta B)^2}{(\alpha^2 + \beta^2)(A^2 + B^2)} \\ &< 1 \end{aligned}$$

as required.

Thus, the Douglas-Rachford algorithm using Schwarzian reflections applied near a simple intersection of two plane analytic curves yields a sequence of iterates that exponentially spirals to the intersection point.

The astute reader will see that if we employ Euclidean reflections in the Douglas-Rachford algorithm our techniques and results still apply and, provided we move to a multi-set version of the Douglas-Rachford algorithm (see for example [5]), readily extend to a family of curves in higher dimensional space, where each curve is specified as an intersection of hyper-surfaces. In this case local convergence is assured by arguments similar to those found in [3]. The reversion to Euclidean reflections is necessary as Schwarzian reflection for curves in a space of dimension greater than two is no longer defined.

3. ALTERNATE APPROACHES TO THE PROBLEM

One ‘‘classical’’ approach to finding an intersection of two implicitly specified plane analytic curves; $f(x, y) = 0$ and $g(x, y) = 0$ would be to compute a zero of

$$(3.1) \quad F : \mathbb{R}^2 \rightarrow \mathbb{R}^2 : (x, y) \mapsto (f(x, y), g(x, y)),$$

using, for instance, Newton’s method.

An alternative approach is to seek solutions of

$$G(f(x, y), g(x, y)) = 0,$$

where $G : \mathbb{R}^2 \rightarrow \mathbb{R}$ is any function vanishing only at $(0, 0)$. We will use $G(u, v) := u^2 + v^2$. Then the problem becomes to locate the global minimum of $G(x, y) = f(x, y)^2 + g(x, y)^2$ (where the function is 0 in the feasible case) For this formulation the method of gradient descent is available, with a line search being implemented at each iteration. Alternatively one could use Newton’s method to find where $\nabla G(x, y) = 0$.

4. EXPERIMENTAL RESULTS

In this section we compare computational results for three test scenarios: two intersecting circles, an ellipse and line, and finding a zero of a function $y = \phi(x)$ which we think of as finding an intersection of the curves $f(x, y) := y - \phi(x) = 0$ and $g(x, y) := y = 0$. In each case we seek to solve the problem using the methods listed in figure 3 for a selection of initial points $P = (p, q)$ chosen to best illustrate different behaviours.

Method Name	Description
DR Euclidean	Douglas-Rachford with Euclidean: $T_{\mathcal{G}_f\mathcal{G}_g} = \frac{1}{2}(I + R_{\mathcal{G}_g}R_{\mathcal{G}_f})$ where $R_{\mathcal{G}_f} = 2P_{\mathcal{G}_f} - I$ with $P_{\mathcal{G}_f}$ the Euclidean projection onto \mathcal{G}_f and similarly for \mathcal{G}_g
DR Schwarzian	Douglas-Rachford using Schwarzian reflection: $T_{\mathcal{G}_f\mathcal{G}_g} = \frac{1}{2}(I + R_{\mathcal{G}_g}R_{\mathcal{G}_f})$ where $R_{\mathcal{G}_f}$ is the Schwarzian reflection in \mathcal{G}_f and similarly for \mathcal{G}_g
Newton on F	Newton's Method applied to find a zero of $F := (x, y) \rightarrow (f(x, y), g(x, y))$
Newton on ∇G	Newton's Method applied to find a zero of ∇G , $G(x, y) = f(x, y)^2 + g(x, y)^2$
Gradient Descent	Gradient Descent with step size determined by a line search, applied to minimize $G(x, y) = f(x, y)^2 + g(x, y)^2$

FIGURE 3. Iterative Methods used on test scenarios.

Colour versions of the diagrams appearing below plus additional details concerning the calculations may be accessed at: <https://carma.newcastle.edu.au/DRmethods/Schwarzian/>.

4.1. Two circles. We consider the circles specified by $f(x, y) := x^2 + y^2 - 1 = 0$ and $g(x, y) := (x - 2)^2 + y^2 - 9/4 = 0$. The intersection points are $(11/16, \pm 3\sqrt{15}/16)$.

In order to see the relative performance of each Douglas-Rachford scheme (Schwarzian versus Euclidean reflections) we plot a fine grid of starting points, each coloured according to the ratio of the number of iterates required by the two schemes to fall within a specified threshold distance from a feasible point. The result is seen in figure 4 where a threshold distance of $1/400$ (half a pixel width) was used and computations were performed to double precision (64 bits, or approximately 15 decimal digits).

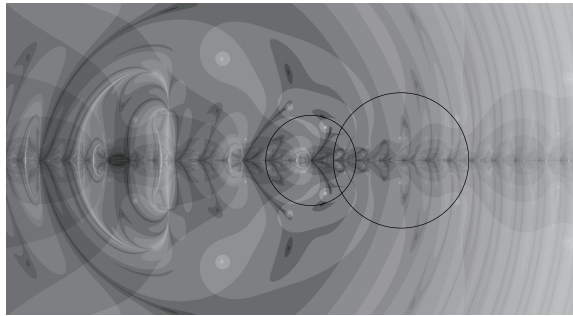


FIGURE 4. Relative performance of the Euclidean and Schwarzian Douglas-Rachford for two circles.

Relative performance of the two schemes are represented on a grey scale with white indicating points where the ratio of “Schwarzian” iterations to “Euclidean”

iterations needed is close to 0 and black where the reciprocal ratio is close to 0. We see that for many points (mid-grey) there is little difference between the performance of the two schemes, nevertheless a rich and interesting pattern is revealed.

Motivated by figure 4 we chose as starting points: $P_1 = (0.31, 0.725)$, $P_2 = (0.41565, 0.62135)$, $P_3 = (-1.81, 0.066)$ and $P_4 = (-4.0556, 0.4471)$. Each pair (P_1, P_2) , (P_3, P_4) includes a point for which the Euclidean scheme performs better, and a point for which the Schwarzian scheme performs better.

Note that the first iteration of Newton's method applied to $F : (x, y) \mapsto (f(x, y), g(x, y))$ moves any initial point P onto the line $x = 11/16$, and each subsequent iteration remains on the line.

The results for the starting points P_1 and P_2 are shown in figure 5 and figure 6 respectively. These points are both close to one of the feasible points, and also close to each other.

	10^{-2}	10^{-3}	10^{-4}	10^{-5}	10^{-6}	10^{-7}	10^{-8}	10^{-9}
DR Euclidean	3	4	6	8	9	11	13	14
DR Schwarzian	1	1	3	5	6	8	10	11
Newton on F	2	3	3	4	4	4	4	4
Newton on ∇G	2	3	3	4	4	4	4	5
Gradient Descent	2	3	4	5	6	6	7	8

FIGURE 5. Performance starting from P_1 .

	10^{-2}	10^{-3}	10^{-4}	10^{-5}	10^{-6}	10^{-7}	10^{-8}	10^{-9}
DR Euclidean	1	1	1	1	3	5	6	8
DR Schwarzian	2	4	6	7	9	11	12	14
Newton on F	2	3	3	3	4	4	4	4
Newton on ∇G	2	3	3	4	4	4	4	4
Gradient Descent	3	4	6	8	9	10	12	14

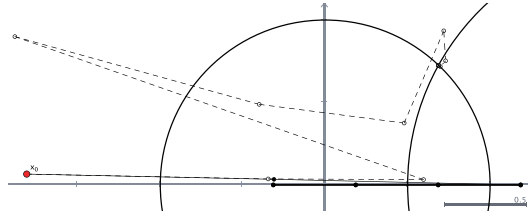
FIGURE 6. Performance starting from P_2 .

Starting from P_1 we see that for thresholds up to 10^{-6} the Schwarzian Douglas-Rachford scheme is roughly twice as fast as the Euclidean Douglas-Rachford scheme, although for smaller thresholds the distinction is less stark. In contrast, starting from P_2 the Euclidean Douglas-Rachford is at least twice as fast as the Schwarzian Douglas-Rachford scheme for thresholds up to 10^{-8} , and often faster. We also note that in both these cases Newton's method is superior to both Douglas-Rachford schemes, while gradient descent is comparable.

With P_3 as starting point Schwarzian Douglas-Rachford drastically outperforms the Euclidean scheme, see figure 7.

The failure of the Euclidean Douglas-Rachford scheme can be seen in figure 8 where the iterates appear to converge to a period 4 point. Observe that a simple calculation for the Euclidean Douglas-Rachford operator $T = T_{G_f G_g}$ and $P = (p, 0)$, where $0 < p < 3/2$, shows that $T^4(P) = P$.

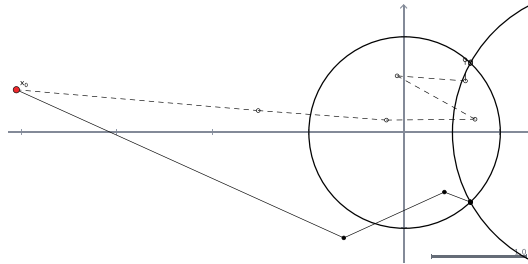
	10^{-2}	10^{-3}	10^{-4}	10^{-5}	10^{-6}	10^{-7}	10^{-8}	10^{-9}
DR Euclidean	Fails to converge in 10000 iterations							
DR Schwarzian	9	10	12	14	15	17	19	20
Newton on F	9	10	10	10	10	11	11	11
Newton on ∇G	Fails to converge in 10000 iterations							
Gradient Descent	4	6	8	10	12	14	16	17

FIGURE 7. Performance for starting point P_3 .FIGURE 8. Douglas-Rachford with starting point $x_0 = P_3$. Euclidean version (solid line) converges to a period 4 point while Schwarzian version (dashed line) converges to a feasible point.

	10^{-2}	10^{-3}	10^{-4}	10^{-5}	10^{-6}	10^{-7}	10^{-8}	10^{-9}
DR Euclidean	3	3	3	4	6	7	9	11
DR Schwarzian	8	9	11	13	14	16	18	19
Newton on F	8	9	9	9	9	10	10	10
Newton on ∇G	8	8	9	9	9	10	10	10
Gradient Descent	4	5	7	8	10	12	13	15

FIGURE 9. Performance for starting point P_4 .

Figure 9 shows the results starting from P_4 . Here Euclidean Douglas-Rachford significantly outperforms the Schwarzian version at all thresholds. We also note that the two schemes converge to different feasible points, see figure 10.

FIGURE 10. Douglas-Rachford with starting point $x_0 = P_4$. Euclidean version (solid line) converges to one feasible point while Schwarzian version (dashed line) converges to the other feasible point.

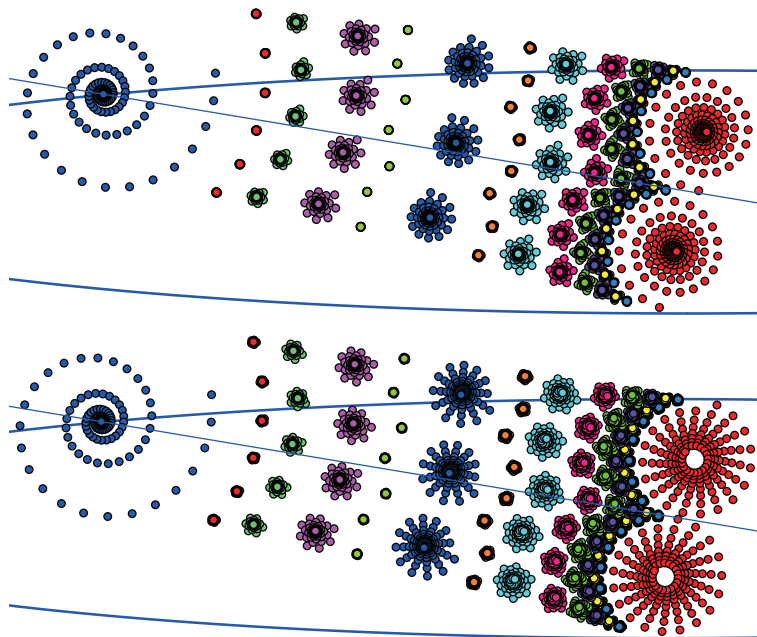


FIGURE 11. Periodic points and their attractive basins for Douglas-Rachford with an ellipse and line with Euclidean Reflection (top) and Schwarzian Reflection (bottom); images have been rotated through 90 degrees.

4.2. Ellipse line. We consider the ellipse $f(x, y) := x^2 + (y/8)^2 - 1 = 0$ and line $g(x, y) := y - 6x = 0$. Starting from anywhere near the ellipse the behaviour of the Schwarzian formulation of Douglas-Rachford appears quite similar to that of the Euclidean formulation. As discussed in [3], for Douglas-Rachford using Euclidean reflection, periodic points appear surrounded by basins of attraction or repulsion. This prevents convergence to the feasible points for many starting points and slows the convergence for many others. We observe the same phenomenon when Schwarzian reflection is employed, where, at least for this particular ellipse and line, the exact same periodic points are observed. This is shown in figure 11. Note that the subsequences have been started from different points in order to illustrate the different sizes of the local basins.

Behaviour of the different methods is tabulated in figure 12.

Locally the behaviour of the two formulations of Douglas-Rachford are nearly identical, however, for more remote starting points, while continuing to converge, the two Douglas-Rachford schemes behave differently and, as in the two circle case may converge to different feasible points.

Remark 4.1. To better assess the effect of compounding numerical error on Douglas-Rachford using Euclidean reflection, where each iteration involves the numerical solution of a Lagrange multiplier problem to find the Euclidean (nearest point) projection $P_{\mathcal{G}_f}$, we experimented with a further variant. For $z \in \mathbb{C}$ we computed $Q_{\mathcal{G}_f}(z)$,

	10^{-1}	10^{-2}	10^{-3}	10^{-4}	10^{-5}	10^{-6}	10^{-8}
DR Euclidean	61	129	197	265	334	402	538
DR Schwarzian	61	129	197	265	334	401	537
Newton on F	2	3	3	4	4	4	4
Newton on ∇G	3	4	4	5	5	5	5
Gradient Descent	2	4	4	6	8	10	12

FIGURE 12. Performance with $f(x, y) = x^2 + (y/8)^2 - 1$, $g(x, y) = y - 6x$, and starting point $(1.5, 4.5)$.

the nearest intersection of \mathcal{G}_f with the line segment from z to its Schwarzian reflection $R_{\mathcal{G}_f}(z)$ and used this as a substitute for $P_{\mathcal{G}_f}(z)$, thereby avoiding the need for a computationally expensive numerical minimisation. Douglas-Rachford was then implemented using $2Q_{\mathcal{G}_f} - I$ as a replacement for reflection in \mathcal{G}_f . Started sufficiently near a feasible or periodic point this yielded nearly identical results to the Euclidean version even after hundreds of iterations. This lack of deviation speaks to the low numerical sensitivity of the Douglas-Rachford method.

4.3. Finding a zero of $y = \phi(x)$. Thinking of this as finding an intersection of the curve $f(x, y) := y - \phi(x) = 0$ with $g(x, y) := y = 0$ leads, via (3.1), to finding a zero of

$$F : \mathbb{R}^2 \rightarrow \mathbb{R}^2 : (x, y) \mapsto (f(x, y), g(x, y)) := (y - \phi(x), y).$$

The Jacobian is

$$J(F) = \frac{\partial(f, g)}{\partial(x, y)} = \begin{pmatrix} -\phi'(x) & 1 \\ 0 & 1 \end{pmatrix}.$$

So, applying Newton's method with any initial point (x_0, y_0) leads to the iterative scheme,

$$x_{n+1} = x_n - \phi(x_n)/\phi'(x_n). \quad y_{n+1} = 0,$$

which, not surprisingly, we recognise as Newton-Raphson applied directly to $y = \phi(x)$.

Thus, for $\phi(x) = x/\sqrt{|x|}$ with any starting point other than $(0, 0)$ this approach leads to cyclic iterates of period 2, and so fails to converge to the zero. By contrast, Douglas-Rachford applied to the two curve reformulation (see discussion below) is seen to rapidly spiral to $(0, 0)$ and to drastically outperform the method of gradient descent applied to the function $G(x, y) = \left(y - x/\sqrt{|x|}\right)^2 + y^2$. The results with initial point $(1, 0)$ are tabulated in figure 13.

Starting from $(1, 0)$ gradient descent does not converge to within 10^{-3} after 20,000 iterations. This may be understood from the shape of the surface $z = G(x, y)$, illustrated in figure 14. Convergence down the sides of the trough is quite rapid, but once near the sharply creased bottom the iterates bounce from side to side making only slow progress toward the minimum.

A more large scale view, starting from the point $(250, 500)$, is provided in figure 15. Here the Schwarzian formulation of Douglas-Rachford requires 293 iterations to come within 10^{-1} of the feasible point while the Euclidean formulation needs 715 iterations.

	10^{-1}	10^{-2}	10^{-3}	10^{-4}	10^{-5}	10^{-6}	10^{-8}	
DR Euclidean	4	4	5	5	6	6	6	
DR Schwarzian	4	5	5	6	6	7	7	
Newton on F	cycles							
Newton on ∇G	fails							
Gradient Descent	4	415						

FIGURE 13. Locating the zero of $y = x/\sqrt{|x|}$ by the methods discussed starting from $(1, 0)$.

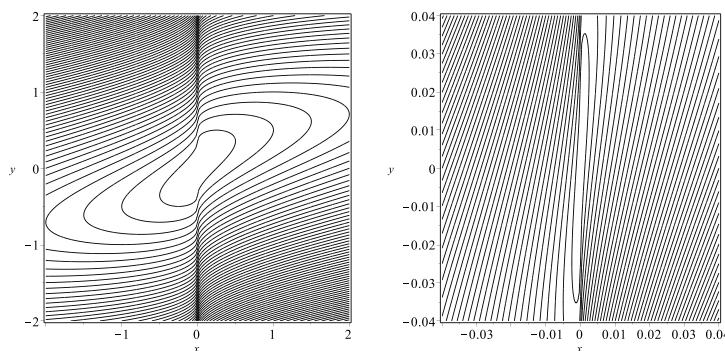


FIGURE 14. The surface $z = G(x, y) = \left(y - x/\sqrt{|x|}\right)^2 + y^2$.

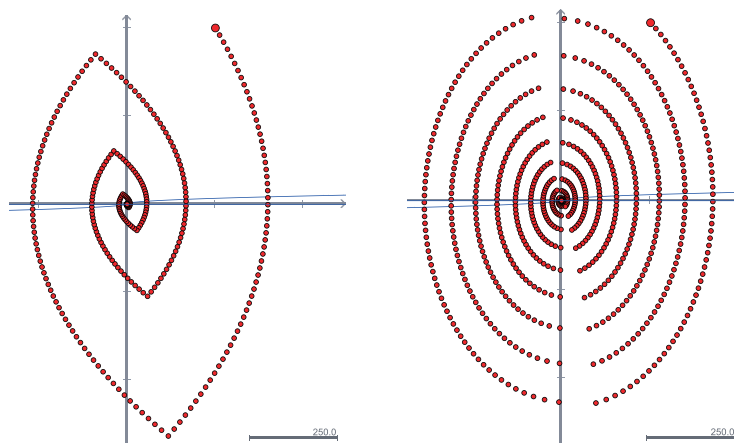


FIGURE 15. Douglas-Rachford applied to the curve $y - x/\sqrt{|x|} = 0$ and line $y = 0$ using Schwarzian reflection (left) and Euclidean reflection (right).

Note: To compute Schwarzian reflection in the curve $\mathcal{C} := \{(x, y) : y = x/\sqrt{|x|}\}$ we write $\mathcal{C} = \mathcal{C}_+ \cup \mathcal{C}_-$, where

$$\mathcal{C}_+ = \{(x, y) : x \geq 0, y = \sqrt{x}\} \quad \text{and} \quad \mathcal{C}_- = \{(x, y) : x \leq 0, y = -\sqrt{-x}\}.$$

Then, if $d(z, \mathcal{C}_+) \geq d(z, \mathcal{C}_-)$ we take $R_{\mathcal{C}}(z) = R_{\mathcal{C}_+}(z) = 1 - z + \sqrt{1 - 4z}$, otherwise we take $R_{\mathcal{C}}(z) = R_{\mathcal{C}_-}(z) = 1 + z - \sqrt{1 + 4z}$.

5. CONCLUSION

While the local similarity of Douglas-Rachford using a Schwarzian reflection and a Euclidean reflection near a feasible point is to be expected, the extent of the similarity is fascinating to observe. Equally fascinating are the large scale differences. Clearly the intersection of complex analysis with iterative methods is a fruitful one. Douglas-Rachford based on Schwarzian reflections often equals or outperforms the same method using Euclidean reflections for the class of problems considered here, and both methods sometimes outperform gradient descent algorithms. In well conditioned problems the quadratic rate of convergence exhibited by Newton's method easily outstrips the linear rate anticipated for projection methods [7]. However, in situations where Newton's method cycles or diverges Douglas-Rachford often continues to work well; this demonstrates the robustness of the algorithms, and Douglas-Rachford using Schwarzian reflection is seemingly the more robust.

The authors wish to acknowledge the late Jonathan Borwein whose work on projection methods provided inspiration for many of the ideas in this note.

REFERENCES

- [1] F. J. Aragón Artacho, J. M. Borwein and M. K. Tam, *Douglas-Rachford feasibility methods for matrix completion problems*, ANZIAM J. **55** (2014), 299–326.
- [2] H. H. Bauschke, P. L. Combettes and D. R. Luke, *Phase retrieval, error reduction algorithm, and Fienup variants: a view from convex optimization*, J. Opt. Soc. Amer. A **19** (2002), 1334–1345.
- [3] J. M. Borwein, S. B. Lindstrom, B. Sims, M. Skerritt and A. Schneider, *Dynamics of the Douglas-Rachford Method for Ellipses and p-Spheres*. (Preprint.)
- [4] J. M. Borwein and B. Sims, *The Douglas-Rachford algorithm in the absence of convexity*, in: Fixed-Point Algorithms for Inverse Problems in Science and Engineering, Springer Optimization and its Applications vol. 49, Springer, 2011, pp. 93–109.
- [5] J. M. Borwein and M. K. Tam, *A cyclic Douglas-Rachford iteration scheme*, J. Optim. Theory Appl. **160** (2014), 1–29.
- [6] P. J. Davis, *The Schwarz Function and its Applications*, Carus Mathematical Monographs, vol. 17, MAA, 1974.
- [7] F. Deutsch, *Rate of convergence of the method of alternating projections*, in: *Parametric Optimization and Approximation*, B. Brosowski and F. Deutsch (eds), Birkhäuser, Basel, 1983, pp. 96–107.
- [8] J. Douglas and H. H. Rachford, *On the numerical solution of the heat conduction problem in 2 and 3 space variables*, Trans. Amer. Math. Soc. **82** (1956), 421–439.
- [9] V. Lakshmikantham and D. Trigiante, *Theory of Difference Equations - Numerical Methods and Applications*, Marcel Dekker, 2002.
- [10] P. L. Lions and B. Mercier, *Splitting algorithms for the sum of two nonlinear operators*, SIAM J. Numer. Anal. **16** (1979), 964–979.
- [11] T. Needham, *Visual Complex Analysis*, Clarendon Press, Oxford, 1997.

Manuscript received ,
revised ,

SCOTT B. LINDSTROM
CARMA, University of Newcastle, Australia
E-mail address: `scott.lindstrom@uon.edu.au`

BRAILEY SIMS
CARMA, University of Newcastle, Australia
E-mail address: `brailey.sims@newcastle.edu.au`

MATTHEW P. SKERRITT
CARMA, University of Newcastle, Australia
E-mail address: `matthew.skerritt@uon.edu.au`